Mater Renew Sustain Energy (2014) 3:31
DOI 10.1007/s40243-014-0031-8

ORIGINAL PAPER

Microstructure and thermoelectric properties of $Y_xAl_yB_{14}$ samples fabricated through the spark plasma sintering

Satofumi Maruyama · Toshiyuki Nishimura · Yuzuru Miyazaki · Kei Hayashi · Tsuyoshi Kajitani · Takao Mori

Received: 3 November 2013 / Accepted: 1 May 2014 / Published online: 27 May 2014

Abstract Excellent control in p- and n-type transport characteristics was previously obtained for the thermoelectric $Y_xAl_yB_{14}$ compounds through Al flux method. In this study, new attempts were made to reduce their grain sizes to obtain dense samples and to possibly lower the thermal conductivity. Introducing the reduction of grain sizes into $Y_xAl_yB_{14}$ samples was attempted by two methods; one was through mechanical grinding, and the other was by synthesizing $Y_xAl_yB_{14}$ via $Y_{0.56}B_{14}$ (denoted as "vYB-YAlB$_{14}$"). Mechanical grinding using ball milling with Si_3N_4 pots and balls was found not to be an efficient way to decrease the grain size because of contamination of Si_3N_4. In contrast, vYB-YAlB$_{14}$ samples were successfully synthesized. Through the synthesis of $Y_{0.56}B_{14}$, the boron network structure was first formed. Afterward, $Y_xAl_yB_{14}$ was obtained by adding Al in the boron network structure through a heat treatment. Due to shorter heating time at lower temperature, the grain sizes were discovered to be smaller than that of Al flux method. The decrease of grain size was found to be beneficial for the densification of $Y_xAl_yB_{14}$ and the decrease of its thermal conductivity.

S. Maruyama · T. Nishimura · T. Mori
International Center for Materials Nanoarchitectonics (MANA), National Institute for Materials Science (NIMS), 1-1 Namiki, Tsukuba 305-0044, Japan

S. Maruyama · Y. Miyazaki · K. Hayashi · T. Kajitani
Department of Applied Physics, Graduate School of Engineering, Tohoku University, 6-6-05 Aoba, Aramaki, Aoba-ku, Sendai 980-8579, Japan

T. Mori (✉)
University of Tsukuba, 1-1-1 Tennodai, Tsukuba, Ibaraki 305-8577, Japan
e-mail: MORI.Takao@nims.go.jp

Keywords Thermoelectric · Boride · n-type · Thermal conductivity · Grain size

Introduction

The development of thermoelectric materials has recently been carried out with great intensity because of the possibility for useful energy conversion of waste heat [1]. Thermoelectric performance is evaluated by the dimensionless figure of merit $ZT = S^2T/\rho\kappa$, where S, ρ, κ and T are the Seebeck coefficient, the electrical resistivity, the thermal conductivity and the absolute temperature, respectively. Boron icosahedra cluster compounds are good candidates for high-temperature thermoelectric materials because they exhibit intrinsic low thermal conductivity and are stable at high temperature [2–5]. Boron carbide is one of the attractive p-type thermoelectric materials for the high-temperature region [6]. Metal doped β-boron compounds have been also investigated as possible thermoelectric materials [7, 8]. In addition, novel boron icosahedra cluster compounds like $RB_{44}Si_2$ (R = rare earth) [9–12], B_6S_{1-x} [13] are being investigated. Rare earth borocarbonitrides, $RB_{22}C_2N$, $RB_{17}CN$ and $RB_{28.5}C_4$, were discovered to be the first boron icosahedra cluster containing compounds that exhibit intrinsic n-type thermoelectric materials [14, 15]. Some of the recently discovered novel borides have been found not to be easy to obtain dense samples, and various studies to remedy this have been carried out; for example, mechanical grinding and sintering the sample through the spark plasma sintering (SPS) treatment with sintering aids such as metals, rare earth tetra brides and carbides [16–19].

Recently, thermoelectric properties of $Y_xAl_yB_{14}$ have been investigated [20] and $Y_xAl_yB_{14}$ was found to exhibit

excellent p–n control with large absolute values of the Seebeck coefficient through the control of the Al occupancy y. To increase figure of merit, we attempt to reduce grain size by means of mechanical grinding and also by a change of synthesis method. The reduction of grain size is expected to help densification of $Y_xAl_yB_{14}$ and decrease thermal conductivity. Since $Y_xAl_yB_{14}$ is usually synthesized with high-temperature molten Al flux method [21], it is normally difficult to reduce the grain sizes through the synthesis conditions. As a result, $Y_xAl_yB_{14}$ is also difficult to densify. Therefore, we focused on the boron atomic network structure of $Y_xAl_yB_{14}$. $Y_{0.56}B_{14}$ (YB_{25}) has a similar atomic network structure and is synthesized by the borothermal reduction [22, 23]. As both compounds have similar boron atomic network structures, we aimed to sinter $Y_xAl_yB_{14}$ via $Y_{0.56}B_{14}$ which possibly can act like a precursor. In this work, we tried to decrease grain size of $Y_xAl_yB_{14}$ samples and investigate effects of the grain size on the thermoelectric properties.

Experiment

Polycrystalline samples of $Y_xAl_yB_{14}$ were synthesized using two methods: one is the high-temperature Al flux method [20, 21] with mechanical grinding using ball milling. Starting materials of YB_4, B and excess Al, serving as flux, were mixed and pressed using cold isostatic pressing. This mixture was heated around 1,633 K. After heating, sample was crushed in a Si_3N_4 mortar and excess Al was dissolved using NaOH. This sample was denoted as "$YAlB_{14}$.'' The $YAlB_{14}$ sample was crushed by ball mill at 200 rpm for 30 min putting balls and ethanol together into a Si_3N_4 pot. This mechanical grinded sample was denoted as "MG-$YAlB_{14}$.'' Another method was the synthesis of $Y_xAl_yB_{14}$ via $Y_{0.56}B_{14}$ (denoted as "vYB-$YAlB_{14}$"). To prevent grain growth through the Al flux method, we sintered $Y_{0.56}B_{14}$ that has a similar crystal structure with $Y_xAl_yB_{14}$, and then Al was added to $Y_{0.56}B_{14}$. Synthesis of $Y_{0.56}B_{14}$ has previously been reported by the borothermal reduction in vacuum as follows [22, 23];

$$Y_2O_3 + (2n+3)B \rightarrow 2YB_n + 3BO.$$

After synthesis of $Y_{0.56}B_{14}$, Al was added to $Y_{0.56}B_{14}$ and the mixture was heated around 1,573 K for 4 h in vacuum. After heating, samples were crushed in a S_3N_4 mortar and excess Al was dissolved using NaOH. All samples were pressed and compacted using SPS treatment at several sintering temperature ranged from 1,673 to 1,823 K.

X-ray diffraction (XRD) measurements using Rigaku Ultima-3 with Cu Kα radiation were performed to characterize the samples and to determine the detailed crystal structure by means of Rietveld refinement using Rietan-FP software [24]. Grain sizes of samples before SPS treatment were checked using a laser diffraction particle size analyzer. The microstructures of the SPS sintered samples are observed using a scanning electron microscope (SEM). The electrical resistivity and the Seebeck coefficient were measured with an ULVAC ZEM-2 using the four-probe method and differential method, respectively. To determine the thermal conductivity, the thermal diffusivity coefficients were measured by the laser flash method and the specific heat was measured by Quantum Design, PPMS.

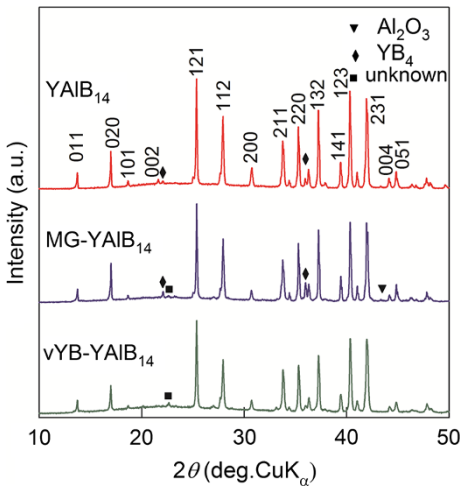

Fig. 1 XRD patterns of $YAlB_{14}$, MG-$YAlB_{14}$ and vYB-$YAlB_{14}$ after SPS treatment. Peak indexes are labeled to main peaks that are isolated or with strong intensities as some peaks are overlapped each other

Result and discussion

XRD patterns of $YAlB_{14}$, MG-$YAlB_{14}$ and vYB-$YAlB_{14}$ samples after SPS treatment are shown in Fig. 1. In the XRD patterns of MG-$YAlB_{14}$ and vYB-$YAlB_{14}$ samples, a small unknown peak was observed around 22.6°. It is considered to be attributed to a very small amount of an unknown secondary phase. In the XRD pattern of Fig. 1, through the ball milling treatment, any secondary phases from the material of the pots or balls were not observed. Although a very small unknown peak was detected, the vYB-$YAlB_{14}$ samples were successfully synthesized. According to the Rietveld analysis, the composition of vYB-$YAlB_{14}$ was $Y_{0.54}Al_{0.59}B_{14}$ and it was almost the same as $YAlB_{14}$ and MG-$YAlB_{14}$ whose composition was estimated at $Y_{0.56}Al_{0.57}B_{14}$. In Fig. 1, the MG-$YAlB_{14}$ sample was observed to have a slight amount of a secondary phase of Al_2O_3. We surmise that during the mechanical grinding, the sample might have been oxidized and Al_2O_3 subsequently appears through the SPS treatment.

The dispersion of the grain sizes are shown in Fig. 2. Before mechanical grinding, the dispersion was broad and

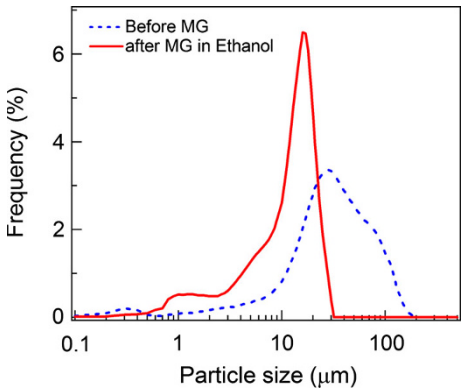

Fig. 2 Dispersion of grain sizes before and after the mechanical grinding

grain size of 50 % of cumulative diameter by the volume grain size distribution (d50) was 28 μm. Through the mechanical grinding treatment at 200 rpm for 30 min, the dispersion became sharper and the grain size of d50 decreased to 12 μm. To decrease grain size further, rotation speed and grinding time were increased. However, with the increase of these parameters, a secondary phase of Si_3N_4 appeared. During the SPS treatment, Si_3N_4 reacted with $Y_xAl_yB_{14}$ and the Al occupancy decreased. As the Al occupancy is strongly related to the thermoelectric properties, the Si_3N_4 contamination should be avoided. Thus, we could not increase the rotation speed and grinding time further.

SEM images of SPS sintered MG-$YAlB_{14}$ and vYB-$YAlB_{14}$ samples are shown in Fig. 3. MG-$YAlB_{14}$ samples in Fig. 3a, b are sintered at 1,773 and 1,823 K under pressure of 150 MPa, respectively. Although the observed grain sizes in Fig. 3a, b were almost same size around 10 μm, grain boundaries disappeared in Fig. 3b and the sintering was largely promoted by the increase of the SPS sintering temperature. This implies that higher sintering temperature leads to densify the samples.

The SEM image of vYB-$YAlB_{14}$ sample after SPS treatment is shown in Fig. 3c. There can be observed some agglomeration of grains and also pores. Through the SPS treatment, the agglomeration was sintered preferentially. To achieve further dense and homogeneous sample, agglomeration should be avoided. Interestingly, the observed average grain size was around 5 μm, which was smaller than those of MG-$YAlB_{14}$ samples. This result can be explained by considering the synthesis route. In the synthesis of the $YAlB_{14}$, we used the Al flux, which was assumed to promote grain growth. In fact, the grain size of d50 of the $YAlB_{14}$ before mechanical grinding was 28 μm as shown in Fig. 2. Even after the mechanical grinding, the grain size of d50 was 12 μm. However, in the synthesis method of the vYB-$YAlB_{14}$ sample, the boron network

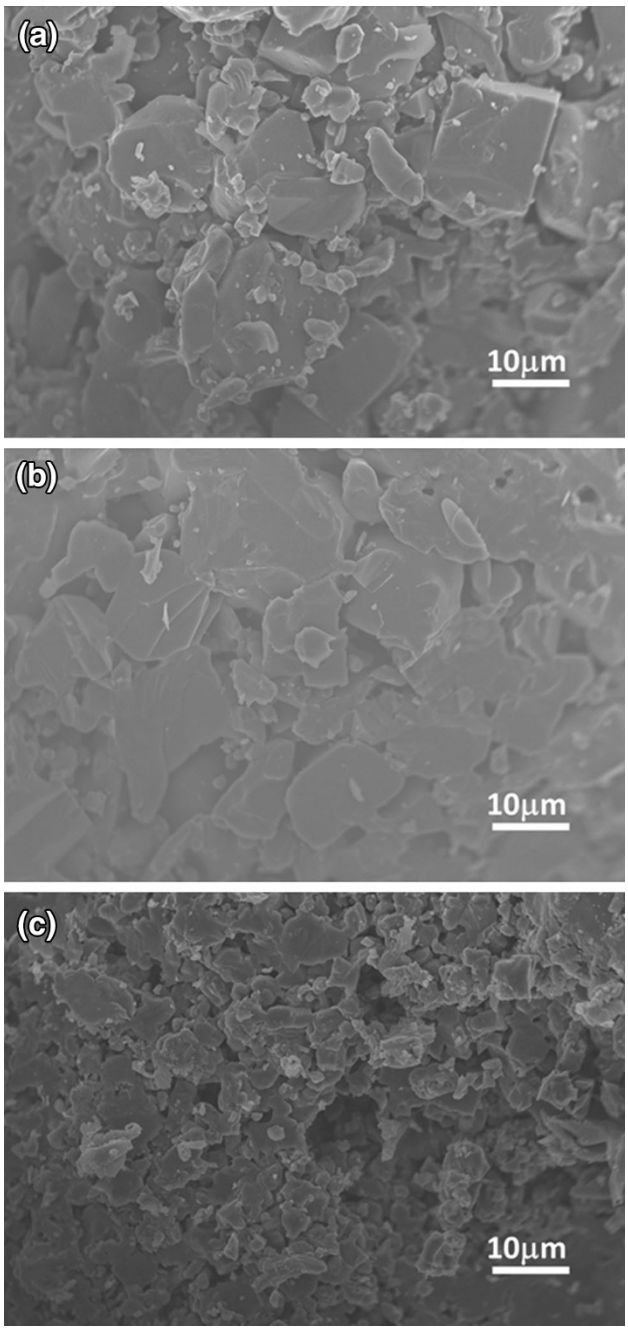

Fig. 3 SEM images of MG-$YAlB_{14}$ samples sintered at 1,773 K **a** and 1,823 K **b** and vYB-$YAlB_{14}$ sintered at 1,673 K **c** after SPS treatment

structure was first formed through the synthesis of $Y_{0.56}B_{14}$, and then afterward, Al was added to the boron network structure through a heat treatment. Since the heat treatment was of shorter time and lower temperature comparing to the Al flux method, we surmise that grain growth of vYB-$YAlB_{14}$ sample was suppressed. Although we could not measure dispersion of the grain sizes of vYB-$YAlB_{14}$ due to the agglomeration, the grain size of the

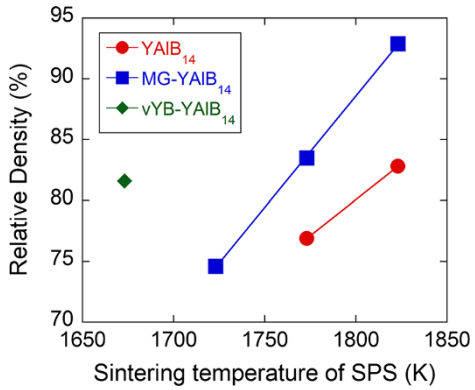

Fig. 4 SPS temperature dependence of the relative density of $YAlB_{14}$, MG-$YAlB_{14}$ and vYB-$YAlB_{14}$ samples

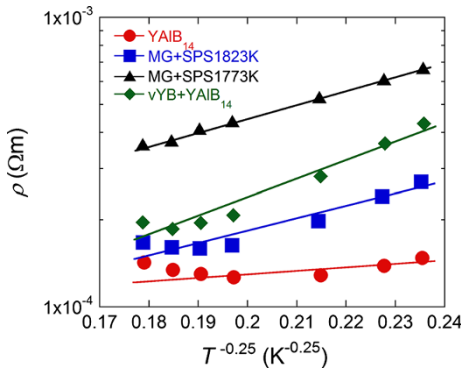

Fig. 5 Temperature dependence of the electrical resistivity of $YAlB_{14}$, MG-$YAlB_{14}$ and vYB-$YAlB_{14}$ samples. The logarithmic of ρ is plotted versus $T^{-0.25}$. The *lines* are guides to the eye

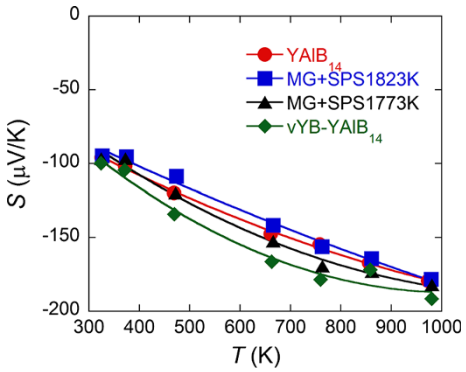

Fig. 6 Temperature dependence of the Seebeck coefficient of $YAlB_{14}$, MG-$YAlB_{14}$ and vYB-$YAlB_{14}$ samples

$vYB\text{-}YAlB_{14}$ seemed to be smaller than that of the $YAlB_{14}$ sample.

The relationship between relative densities of samples and SPS sintering temperature is plotted in Fig. 4. The relative density of the $YAlB_{14}$ samples was increased with increasing the SPS sintering temperature and reached 83 % at 1,823 K without special treatment for reducing grain sizes. In MG-$YAlB_{14}$ samples, relative densities were also largely increased with the increase of the SPS sintering temperature. In addition, compared to the $YAlB_{14}$ sample, sample density was largely increasing from 83 to 93 % at 1,823 K. For the vYB-$YAlB_{14}$ sample, relative density was 82 % even for the lower SPS sintering temperature at 1,673 K and almost as same relative density as $YAlB_{14}$ sample sintered at 1,823 K. With the decrease of the grain sizes, relative densities tend to increase and sintering temperature tend to become lower, due to the increase of the specific surface area of the samples. Therefore, from our results, we can conclude that the decrease of the grain size leads to lower the SPS temperature to obtain dense $Y_xAl_yB_{14}$ samples.

The temperature dependence of electrical resistivity of samples is shown in Fig. 5. The electrical resistivity of $Y_xAl_yB_{14}$ was previously observed [20] to follow Mott's variable range hopping mechanism, $\log\rho \propto T^{-0.25}$ [25, 26]. The temperature dependences of electrical resistivities observed to not follow this dependency and show curvatures due to the existence of grain boundaries, pores and secondary phases. The electrical resistivities of MG-$YAlB_{14}$ samples were higher than that of $YAlB_{14}$ sample in spite of the higher relative density. The MG-$YAlB_{14}$ samples seemed to be oxidized, and this can be considered as one of the reasons for the higher electrical resistivity. The electrical resistivity of the vYB-$YAlB_{14}$ sample was also increasing. According to the SEM image of vYB-$YAlB_{14}$ sample in Fig. 3c, grain boundaries and pores can be observed and they can increase the electrical resistivity.

The temperature dependence of the Seebeck coefficient is shown in Fig. 6. The Seebeck coefficient in variable range hopping has been investigated, for example, by Zvyagin [27]. Assuming linear density of state, the Seebeck coefficient has the following dependency:

$$S \propto (T_0 T)^{1/2} d(\ln \mathrm{D}(E))/dE|_{E_\mathrm{F}}$$

The Seebeck coefficients of samples also tended to be proportional to $T^{1/2}$ and exhibited around -190 μV/K at 1,000 K. Previously, we found the Al occupancies of samples relate with T_0 values [20]. Since the Al occupancies were almost the same value between samples here, little difference of the temperature dependence of the Seebeck coefficient was observed. Although the Seebeck coefficient can be increased through the reduction of the grain size [28, 29], we conclude the Seebeck coefficient is not changed by the reduction of grain sizes among samples obtained in this study.

Thermal conductivities of all samples are plotted in Fig. 7. The thermal conductivity of $YAlB_{14}$ sample was decreasing with the increase of the temperature and exhibited 3.6 W/mK at 1000 K. The thermal conductivity

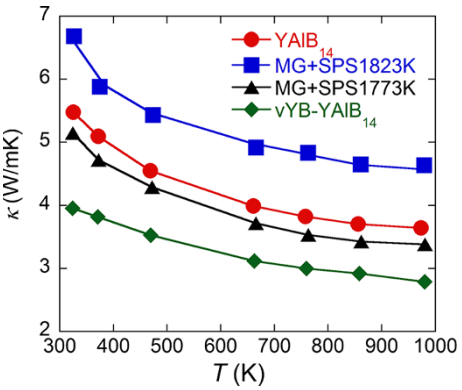

Fig. 7 Temperature dependence of the thermal conductivity of $YAlB_{14}$, MG-$YAlB_{14}$ and vYB-$YAlB_{14}$ samples

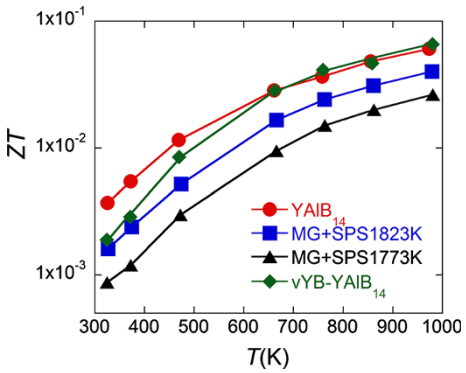

Fig. 8 Temperature dependence of the figure of merits of $YAlB_{14}$, MG-$YAlB_{14}$ and vYB-$YAlB_{14}$ samples

of the MG-$YAlB_{14}$ sample sintered at 1,773 K slightly decreased compared to $YAlB_{14}$ due to the decrease of grain sizes, i.e., the increase of the grain boundary. It leads to increase the phonon scattering and to decrease the thermal diffusivity. On the other hand, the thermal conductivity of the MG-$YAlB_{14}$ sample sintered at 1,823 K was higher than that of $YAlB_{14}$ due to the disappearance of grain boundaries. The thermal conductivity of vYB-$YAlB_{14}$ sample decreased with the increase of the temperature and exhibited 2.8 W/mK at 1,000 K. The thermal conductivity of vYB-$YAlB_{14}$ was the lowest among the samples although the relative density is the same as $YAlB_{14}$ and MG-$YAlB_{14}$ sintered at 1,773 K. The observed decrease of the thermal conductivity is caused by the large reduction in the lattice contribution. Considering both the SEM image and the result of thermal conductivity measurement, we can conclude that the synthesis method of the vYB-$YAlB_{14}$ sample is most effective to increase phonon scattering and to decrease thermal conductivity.

Temperature dependence of *ZT* value is plotted in Fig. 8. The *ZT* value of $YAlB_{14}$ sample increased with the increase of the temperature and exhibited 0.060 at 1000 K. *ZT* values of the MG-$YAlB_{14}$ samples decreased relative to $YAlB_{14}$ due to the decrease of the electrical resistivity, while the thermal conductivity did not decrease largely, because grain sizes were not decreased sufficiently through the mechanical grinding. The *ZT* value of vYB-$YAlB_{14}$ was slightly increasing in high-temperature range and exhibited 0.066 at 1000 K, because the thermal conductivity was decreased. However, as the electrical resistivity of vYB-$YAlB_{14}$ sample increased compared to $YAlB_{14}$ sample, *ZT* value of vYB-$YAlB_{14}$ was not enhanced so much. As we wrote in the parts of the results of the SEM and the electrical resistivity measurements, grain boundaries and pores can be observed in vYB-$YAlB_{14}$ sample. Due to these reasons, the electrical resistivity of vYB-$YAlB_{14}$ increased. Although the increase of *ZT* is within the general error, since the values are those experimentally obtained, the difference can be considered to represent a tendency, at least indicating that the grain size control approach is promising. Although *ZT* values of vYB-$YAlB_{14}$ were still low due to the low density, further improvements are expected through the optimization of the synthesis condition.

Conclusion

In this study, the reduction of grain sizes was introduced to $Y_xAl_yB_{14}$ samples by two methods. One was the mechanical grinding using ball milling with Si_3N_4 pots and balls. However, it was found not to be an efficient way to reduce the grain size because of the contamination of Si_3N_4. Thermoelectric performance of mechanical grinded sample (MG-$YAlB_{14}$) was found not to be improved due to the secondary phase and the insufficiency of the decrease of the grain size. The other was the synthesis of $Y_xAl_yB_{14}$ sample via $Y_{0.56}B_{14}$ (vYB-$YAlB_{14}$). The vYB-$YAlB_{14}$ sample was successfully synthesized, and the grain sizes were discovered to be smaller than that of Al flux method. Considering both MG-$YAlB_{14}$ and vYB-$YAlB_{14}$, it was found that through the reduction of grain sizes, the relative densities after SPS treatment tend to increase at the same SPS sintering temperature. Thermal conductivity of vYB-$YAlB_{14}$ sample was discovered to be the lowest among the samples thanks to the small grain size, i.e., the increase of the grain boundaries. As a result, *ZT* value of vYB-$YAlB_{14}$ sample showed a slight enhancement in the high-temperature region. With further reduction of grain sizes through improvement of the synthesis process of the vYB-AlB_{14} and optimization of SPS conditions to consolidate, further improvements are expected.

Acknowledgments TM was partially supported by a grant from AOARD.

References

1. Koumoto, K., Mori, T.: Thermoelectric Nanomaterials; Materials Design and Applications, Springer Series in Materials Science, vol. 182. Springer, Heidelberg (2013)
2. Mori, T.: Higher borides. In: Gschneidner Jr, K.A., Bunzli, J.-C., Pecharsky, V. (eds.) Handbook on the Physics and Chemistry of Rare-Earths, vol. 38, p. 105. North-Holland, Amsterdam (2008)
3. Slack, G.A., Oliver, D.W., Horn, F.H.: Thermal conductivity of boron and some boron compounds. Phys. Rev. B **4**, 1714–1720 (1971)
4. Cahill, D.G., Fischer, H.E., Watson, S.K., Pohl, R.O.: Thermal properties of boron and boride. Phys. Rev. B **40**, 3254–3260 (1989)
5. Mori, T.: Thermal conductivity of a rare-earth *B*12-icosahedral compound. Phys. B **383**, 120–121 (2006)
6. Wood, C., Emin, D.: Conduction mechanism in boron carbide. Phys. Rev. B **29**, 4582–4587 (1984)
7. Nakayama, T., Shimizu, J., Kimura, K.: Thermoelectric properties of metal-doped β-rhombohedral boron. J. Solid State Chem. **154**, 13–19 (2000)
8. Kim, H., Kimura, K.: Vanadium concentration dependence of thermoelectric properties of β-rhombohedral boron prepared by spark plasma sintering. Mater. Trans. **52**, 41–48 (2011)
9. Mori, T.: High temperature thermoelectric properties of B_{12} icosahedral cluster-containing rare earth boride crystal. J. Appl. Phys. **97**, 093703 (2005)
10. Mori, T., Martin, J., Nolas, G.: Thermal conductivity of $YbB_{44}Si_2$. J. Appl. Phys. **102**, 073510 (2007)
11. Mori, T., Berthebaud, D., Nishimura, T., Nomura, A., Shishido, T., Nakajima, K.: Effect of Zn doping on improving crystal quality and thermoelectric properties of borosilicides. Dalton Trans. **39**, 1027–1030 (2010)
12. Berthebaud, D., Sato, A., Michiue, Y., Mori, T., Nomura, A., Shishido, T., Nakajima, K.: Effect of transition element doping on crystal structure of rare earth borosilicides $REB_{44}Si_2$. J. Solid State Chem. **184**, 1682–1687 (2011)
13. Sologub, O., Matsusita, Y., Mori, T.: An α-rhombohedral boron related compound with sulfur: synthesis structure and thermoelectric properties. Scripta Mater. **68**, 289–292 (2013)
14. Mori, T., Nishimura, T.: Thermoelectric properties of homologous p- and n-type boron-rich borides. J. Solid State Chem. **179**, 2908–2915 (2006)
15. Mori, T., Nishimura, T., Yamaura, K., Takayama-Muromachi, E.: High temperature thermoelectric properties of a homologous series of n-type boron icosahedra compounds: a possible counterpart to p-type boron carbide. J. Appl. Phys. **101**, 093714 (2007)
16. Berthebaud, D., Nishimura, T., Mori, T.: Thermoelectric properties and spark plasma sintering of doped $YB_{22}C_2N$. J. Mater. Res. **25**, 665–669 (2010)
17. Berthebaud, D., Nishimura, T., Mori, T.: Microstructure and thermoelectric properties of dense $YB_{22}C_2N$ samples fabricated through spark plasma sintering. J. Electron. Mater. **40**, 682–686 (2011)
18. Prytuliak, A., Mori, T.: Effect of transition-metal additives on thermoelectric properties of $YB_{22}C_2N$. J. Electron. Mater. **40**, 920–925 (2011)
19. Prytuliak, A., Maruyama, S., Mori, T.: Anomalous effect of vanadium boride seeding on thermoelectric properties of $YB_{22}C_2N$. Mater. Res. Bull. **48**, 1972–1977 (2013)
20. Maruyama, S., Miyazaki, Y., Hayashi, K., Kajitani, T., Mori, T.: Excellent p-n control in a high temperature thermoelectric boride. Appl. Phys. Lett. **101**, 152101 (2012)
21. Korsukova, M.M., Lundstrom, T., Tergenius, L.-E., Gurin, V.N.: The crystal structure of defective $YAlB_{14}$ and $ErAlB_{14}$. J. Alloy Compd. **187**, 39–47 (1992)
22. Tanaka, T., Okada, S., Yu, Y., Ishizawa, Y.: A new yttrium boride: YB_{25}. J. Solid State Chem. **133**, 122–124 (1997)
23. Mori, T., Zhang, F.X., Tanaka, T.: Synthesis and magnetic properties of binary boride REB_{25} compounds. J. Phys.: Condens. Matter **13**, L423–L430 (2001)
24. Izumi, F., Momma, K.: Three-dimensional visualization in powder diffraction. Solid State Phenom. **130**, 15–20 (2007)
25. Efros, A.L., Pollak, M.: Electron–Electron Interactions in Disordered Systems. North-Holland, Amsterdam (1985)
26. Mott, N.F.: Conduction in glasses containing transition metal ions. J. Non-Cryst. Solids **1**, 1–17 (1968)
27. Zvyagin, I.P.: On the theory of hopping transport in disordered semiconductors. Phys. Status Solidi B **58**, 443–449 (1973)
28. Kishimoto, K., Yamamoto, K., Koyanagi, T.: Influences of potential barrier scattering on the thermoelectric properties of sintered n-type PbTe with a small grain size. Jpn. J. Appl. Phys. **42**, 501–508 (2003)
29. Heremans, J.P., Thrush, C.M., Morelli, D.T.: Thermopower enhancement in lead telluride nanostructures. Phys. Rev. B **70**, 115334 (2004)